



UNIVERSITY OF LEEDS

This is a repository copy of *Fabrication of free-standing octagon-shaped carbon nanofibre assembly for electrical actuation of shape memory polymer nanocomposites*.

White Rose Research Online URL for this paper:
<http://eprints.whiterose.ac.uk/91092/>

Version: Accepted Version

Article:

Lu, H, Yao, Y, Zhu, S et al. (2 more authors) (2015) Fabrication of free-standing octagon-shaped carbon nanofibre assembly for electrical actuation of shape memory polymer nanocomposites. *Pigment and Resin Technology*, 44 (3). 157 - 164. ISSN 0369-9420

<https://doi.org/10.1108/PRT-10-2014-0092>

Reuse

Unless indicated otherwise, fulltext items are protected by copyright with all rights reserved. The copyright exception in section 29 of the Copyright, Designs and Patents Act 1988 allows the making of a single copy solely for the purpose of non-commercial research or private study within the limits of fair dealing. The publisher or other rights-holder may allow further reproduction and re-use of this version - refer to the White Rose Research Online record for this item. Where records identify the publisher as the copyright holder, users can verify any specific terms of use on the publisher's website.

Takedown

If you consider content in White Rose Research Online to be in breach of UK law, please notify us by emailing eprints@whiterose.ac.uk including the URL of the record and the reason for the withdrawal request.



eprints@whiterose.ac.uk
<https://eprints.whiterose.ac.uk/>

Fabrication of free-standing octagon-shaped carbon nanofibre assembly for electrical actuation of shape memory polymer nanocomposites

H.B. Lu and Y.T. Yao¹

National Key Laboratory of Science and Technology on Advanced Composites in Special Environments, Harbin Institute of Technology, Harbin 150080, China

S.P. Zhu and Y.H. Yang

Science and Technology on Advanced Functional Composites Laboratory, Aerospace Research Institute of Materials & Processing Technology, Beijing 100076, PR China

L. Lin

Department of Colour and Polymer Chemistry, University of Leeds, Leeds LS2 9JT, UK

Abstract

Purpose – This paper reports a study aimed at overcoming the interface issue between nanopaper and polymer matrix in shape memory polymer (SMP) laminate composites caused by their large dissimilarity in electrical/thermal conductive properties. The study attempted to develop an effective approach to fabricate free-standing carbon nanofibre (CNF) assembly in octagon shape formation. The structure design and thermal conductive performance of the resulting octagon-shaped CNF assembly were optimised and simulated.

Design/methodology/approach – The CNF nanopaper were prepared based on a filtration method. The SMP nanocomposites were fabricated by incorporating these CNF assemblies with epoxy-based SMP resin by a resin-transfer modelling technique. Thermal conductivity of the octagon-shaped CNF assembly was simulated using the ANSYS FLUENT software for structure design and optimisation. The effect of the octagon-shaped CNF on the thermomechanical properties and thermally responsive shape memory effect (SME) of the resulting SMP nanocomposites were characterised and interpreted.

Findings – The CNF template incorporated with SMP to achieve Joule heating triggered shape recovery at a low electric voltage of 3-10 V due to which the electrical resistivity of SMP

¹ Corresponding author; e-mail: yaoyt@hit.edu.cn

nanocomposites was significantly improved and lowered to 0.20 Ω -cm by the CNF template. It was found that the octagon CNF template with 2 mm width of skeleton presented a highest thermally conductive performance to transfer resistive heat to the SMP matrix.

Research implications – A simple way for fabricating electro-activated SMP nanocomposites has been developed by employing octagon CNF template. Low electrical voltage actuation in SMP has been achieved.

Originality/value – The fabricated CNF template, the structure design and analysis of dynamic thermomechanical properties of SMP are novel.

Keywords – Shape memory polymer, Carbon nanofibre, Electrical actuation, Thermal responsive

Paper type Research paper

Introduction

Shape memory polymers (SMPs) having unique shape memory effect (SME) (Bellin *et al.*, 2006; Behl and Lendlein 2007), high elastic strain (Razzaq *et al.*, 2007), tailorable transition temperature (Miaudet *et al.*, 2007; Hu and Chen, 2010), an ease of manufacturing (Li *et al.*, 2000) and variable in mechanical and physical properties (Hollaway 2011; Lu *et al.*, 2013a; Lu *et al.*, 2013b; Lu and Du 2014) are of great interest due to their potential to replace traditional shape memory alloys (SMAs) in both academic research and industrial applications (Gall *et al.*, 2004; Huang *et al.*, 2011). In the past three decades, research on SMPs has resulted in significant number of achievements in the scientific fields, especial in chemistry (Kim *et al.*, 1998; Lendlein 2010; Huang *et al.*, 2010; Mather *et al.*, 2009), materials science (Cho *et al.*, 2005; Lu *et al.*, 2010b; Lu and Gou 2012), physics (Tobushi *et al.*, 2008; Lu *et al.*, 2010a), mechanics (Tobushi *et al.*, 2001; Nguyen *et al.*, 2008), microelectronic engineering (Gall *et al.*, 2004), textile science (Hu *et al.*, 2012) and biomedicine science (Tang *et al.*, 2013; Lendlein, 2002). Consequently, there now exist many types of SMPs, including polyurethane (Tobushi *et al.*, 2008), polyethylene terephthalate (PET) (Li *et al.*, 2009), polyethyleneoxide (Choi *et al.*, 2014), polystyrene (Leng *et al.*, 2009a), epoxy (Dietsch and Tong, 2007) etc. Some of these SMPs have shown high mechanical performance (Yoonessi *et al.*, 2012), while others demonstrated biocompatibility and biodegradability (Yakacki and Shandas 2007), as well as those showing multi-shape memory effect (m-SME) and temperature memory effect (TME) (Sun and Huang, 2010; Xie, 2010; Lu, 2013). These exciting properties and performances help SMPs to be attractive and competitive in “intelligent” or “smart” materials (Paik *et al.*, 2006; Lantada *et al.*, 2010). On the other hand, it was recognised that several drawbacks limited the research and development

of SMPs which included low recovery ratio, output mechanical strength, slow recovery speed etc. (Mather *et al.*, 2009; Sun *et al.*, 2012; Fejos *et al.*, 2012). Almost all of these resulted from the intrinsic nature of polymer. Here, traditional research and development on polymer science and technology provide an effective approach to employ for SMPs. SMP composites and SMP nanocomposites are introduced to conquer the above-mentioned drawbacks and thus retain SMP's competitiveness in comparison with SMAs, according to the researches on polymer composites and polymer nanocomposites (Dong *et al.*, 2013a; Choi *et al.*, 2012; Dong *et al.*, 2013b; Lee and Yu 2011; Lu *et al.*, 2011a; Lu *et al.*, 2011c). Due to such motivations, there has seen publication of significant number of studies on SMPs nanocomposites, in order to achieve their high mechanical performance (Dong *et al.*, 2013a), multi-functionalisation (Choi *et al.*, 2012; Dong *et al.*, 2013b) and various recovery activations (Lee and Yu 2011; Lu *et al.*, 2011a; Lu *et al.*, 2011c). Meanwhile, utilisation of functional filler, such as thermally conductive particle (Maitland *et al.*, 2002; Leng *et al.*, 2009b), electrically conductive particle (Leng *et al.*, 2007; Lu *et al.*, 2011b), or magnetically responsive particles (Mohr *et al.*, 2006), to induce the shape recovery of SMP respectively by infrared radiation, laser light, electrically resistive Joule heating, magnetic field, has provided the composites with tailorable performances and manually designable properties.

Utilisation of electrically resistive Joule heating to trigger the SME is desirable and convenient in some practical applications, especially when direct heating is not easily achievable, particularly in aerospace engineering and aircraft morphing structures (Rousseau 2008; Lan *et al.*, 2009). Remarkable progress in electrical actuation of SMP composites by incorporation of electric particles or fillers has been made via a knowledge-based approach (Leng *et al.*, 2007; Lu *et al.*, 2011b; Luo and Mather 2010; Lu *et al.*, 2011a; Liu *et al.*, 2009; Lu *et al.*, 2014a). Meanwhile, an attractive approach to introduce various forms of film or nanopaper has been recently introduced for electrical actuation of SMP nanocomposites (Luo and Mather 2010; Lu *et al.*, 2011a; Liu *et al.*, 2009; Lu *et al.*, 2014a). Thus, the high viscosity and poor shape recovery performance could be prevented to a certain extent. The interface issue in SMP laminate between the nanopaper and polymer matrix occurred due to their largely dissimilarity in electrical/thermal conductive properties, when the applied voltage was above certain level (Lu and Huang 2013). Therefore, it is essential to optimise the structure of the SMP composite laminate. In the study reported here, an effective approach to fabricate free-standing carbon nanofibre (CNF) assembly into octagon shape formation is reported. In this study, the structure design and thermally conductive performance and of the octagon-shaped CNF template had been initially optimised and simulated. The CNF template had then incorporated with SMP to significantly lower its electrical resistivity and achieve Joule heating

triggered SME upon the application of electric voltage. Finally, the electro-activated recovery behaviour and the resultant temperature distribution within SMP nanocomposite were recorded and monitored to facilitate the structure design and optimisation of the octagon-shaped CNF template. Heat transfer from CNF template to SMP matrix is further discussed with regard to their interfacial issue. Additionally, the effect of CNF template on the dynamic thermomechanical properties and instinctive structure of SMP had also been studied.

Experimental

Methods of preparation of octagon-shaped CNF nanopaper and SMP nanocomposites

The fabrication process of octagon-shaped CNF assembly is similar to that of CNF nanopaper (Li *et al.*, 2009). Thus, 0.6 g raw CNFs were initially dispersed into 600 mL distilled water with the aid of 0.2 mg non-ionic surfactant. And then, the CNF suspension was mechanically stirred and sonicated for 30 minutes at room temperature of 22°C. After that, the CNF suspension was filtered through a 4.5 µm hydrophilic polycarbonate membrane filter that is coated with a metallic octagon-shaped template, under a positive pressure of 60 psi to yield a film. Finally, the CNF assembly was dried in an oven at 120°C for 2 hours to remove remaining water and the surfactant, as shown in Figure 1(a). In this study, the octagon-shaped CNF assembly (see Figure 1(b)) was prepared using a laser cutter. Subsequently, the SMP nanocomposites were fabricated by incorporating these CNF assemblies with epoxy-based SMP resin by resin-transfer modelling technique. After the mould was filled up, the mixture was cured at a temperature ramp of approximately 1°C/min from 25°C to 100°C and kept for 5 hours before being ramped to 120°C at 20°C per 180 minutes. Finally, it was ramped to 150°C to produce the final SMP nanocomposites.

Methods of characterisation

Characterisation of chemical structures of CNF nanopaper and nanocomposites

X-ray diffraction (XRD Empyrean, Pananalytical, Holland) was employed to analysis the effect of CNF assembly on the SMP. The specimens were analysed in the range of 5°-75° with a scanning speed of 5°/min.

Raman spectroscopy (Horiba HR 800 spectrometer) was used to characterise the disorder and defects in CNF. 638 nm radiation from 1 mW air-cooled Argon ion laser was used as exciting source, in a range from 100 to 4000 cm⁻¹.

Dynamic mechanical thermal analysis

Dynamic mechanical analysis (DMA 242C Netzsch, Germany) of pristine epoxy-based SMP and SMP nanocomposites incorporated with octagon-shaped CNF assembly with 0.8 mm and

1.2 mm in thickness was carried out to characterise the dynamic thermomechanical properties. All three SMP nanocomposite specimens with a dimension of $9.00 \times 2.9 \times 0.84 \text{ cm}^3$ were performed in a three-point bending mode at a constant heating rate of $10^\circ\text{C}\cdot\text{min}^{-1}$ and an oscillation frequency of 1 Hz from 25 to 180°C .

Thermal/electrical actuation with temperature sensing

The electrical resistivity of SMP nanocomposites incorporated with octagon-shaped CNF assembly of 0.4, 0.8 and 1.2 mm in thickness was determined as 0.27, 0.22 to 0.20 $\Omega\cdot\text{cm}$, respectively, by the Van der Pauw method. With a low electrical conductivity, the electrical actuation and electrically induced SME of SMP nanocomposite could be achieved by applying a suitable electric current. The tested SMP nanocomposites had a permanent flat shape with a dimension of $60 \times 6 \times 1.2 \text{ mm}^3$. After the nanocomposites were heated above 120°C , it deformed into a "U" shape upon application of an external force. After cooling back to room temperature, the deformed shape remained. A DC electric current was applied to the SMP nanocomposites incorporated with the 2 mm width of skeleton of the octagon-shaped CNF assembly at a porosity of 80%. The electrical actuation and temperature distribution within the tested SMP nanocomposites were recorded by an infrared video camera (VarioCAM HiRes, JENOPTIK Infra Tec.).

Results and discussion

Structure design and fabrication of octagon-shaped CNF assembly

Thermal conductivity of the octagon-shaped CNF assembly is initially simulated by the ANSYS FLUENT software for structure design and optimisation. According to the applied electric current, Figure 1(c) presents the electrically resistive heating flow that results in a temperature distribution within the tested specimen. And the relative thermal conductivity is also simulated according to the temperature distribution within the tested specimen, as shown in Figure 1(d). On the other hand, the relative thermal conductivity of the octagon-shaped CNF assembly (with a variety of width of skeleton) has been analysed and compared to quantitatively separate the effect of porosity ratio on the thermal conductivity, as shown in Figure 2. These simulation results support that the octagon-shaped CNF assembly with 2 mm width of skeleton presents the highest relative thermal conductivity in comparison with that with 1 mm and 3 mm width of skeleton at the same porosity ratio of 80%, 82%, and 84%. On the other hand, it was observed that with the increase of the porosity ratio of octagon-shaped CNF assembly, the effectiveness of electrically resistive heat decreased due to the decrease of the weight ratio of CNF assembly in the SMP nanocomposite. Therefore, the octagon-shaped CNF assembly with 2 mm width of skeleton at a porosity ratio of 80% has been prepared and

used as a basis to improve the electrical and thermal conductivity for SMP matrix in the subsequent work.

(Take in Figure 1)

(Take in Figure 2)

X-ray diffraction (XRD) studies

Analysis via X-ray diffraction (XRD) was carried out to confirm the effect of CNF assembly on the SMP. The XRD pattern obtained showed numbers of Bragg reflections for the face centered cubic structure. The XRD pattern of the epoxy-based SMP and its nanocomposite obtained by mulberry leaves extract is shown in Figure 3. It is found that the pristine SMP was evidenced by the diffuse peaks at 2θ value of 17.6° due to impurities of crystal structure of polymer macromolecules. On the other hand, the CNF assembly enabled SMP nanocomposite was evidenced by the diffuse peaks at 2θ value of 26.4° corresponding to the Bragg reflections of graphite structure of C=C. The X-ray diffraction results show that the nanofibre formed by the mulberry leaves extract are crystalline in nature. The narrow diffraction peak indicates a layer-to-layer distance (d-spacing) of 0.85 nm for the CNF assembly.

(Take in Figure 3)

Raman spectra characterisation

The CNFs could manifest themselves in Raman spectra by means of changing relative intensity of two main peaks: D and G bands. As revealed in Figure 4, there exists the D peak of CNF located at 1337 cm^{-1} from a defect-induced breathing mode of sp^2 rings. Here, Raman spectroscopy is shown to provide a powerful tool to differentiate sp^2 carbon nanostructures of CNFs. The intensity of D band is related to the size of the in-plane sp^2 domains (Choi *et al.*, 2014; Leng *et al.*, 2009a). On the other hand, the G bonding of C=C shifts from 1600 cm^{-1} . The relative intensity ratio of both peaks (I_D/I_G) is a measure of the degree of disorder and is inversely proportional to the average size of the sp^2 clusters (Dietsch and Tong 2007). The D/G intensity ratio for CNF is of 0.83 that is smaller than that of the graphene of 0.85. This suggests that less graphitic domains were formed and the sp^2 cluster number decreased.

(Take in Figure 4)

Dynamic mechanical analysis

The storage modulus and $\tan\delta$ data as a function of temperature of the tested specimens were plotted in Figure 5. As can be seen from Figure 5, the experimental results reveal that the storage modulus were 1889, 2149 and 2614 MPa for the pristine SMP and SMP nanocomposites at 25°C , respectively. Such experimental results imply that the addition of CNFs increases the

storage modulus of nanocomposites over the whole temperature range. The CNF assembly could help polymer matrix to resist external loading due to excellent mechanical properties of the CNFs, resulting in an improved mechanical performance. Furthermore, the glass transition temperature (T_g) is defined as the intersection point of storage modulus and the tangent delta curves. In this manner, the T_g is of 64.5°C, 66.8°C and 75.3°C for the pristine SMP and SMP nanocomposites incorporated with octagon-shaped CNF assembly of 0.8 mm and 1.2 mm in thickness, respectively. Experimental results could be attained from the CNF assembly that enhances the thermomechanical properties of SMP matrix, resulting in improved T_g .

(Take in Figure 5)

Electrical actuation and temperature distribution

Figures 6(a), (b), (c) and (d) present the temperature distribution when the electrodes were connected to the SMP nanocomposite to apply a variety of electric voltages of 3 V, 6 V, 9 V and 10 V, respectively. It was found that the electrically resistive heat results in the temperature increased with an increase in heating time from 0 s to 118 s. The electrically resistive heating transfer in the electric current according to the temperature distribution in the electrical actuation was observed. Thus, after being subjected to the application of the electric voltage of 3 V, 6 V, 9 V and 10 V for 118s, respectively, the SMP nanocomposite were heated up to 53.4, 110.7, 198.8 and 218.8°C, respectively, while a T_g of 75.3°C was determined by DMA analysis. Clearly, as a higher electric voltage was applied on the tested specimen, the electric power increased according to the Ohm's rule.

(Take in Figure 6)

Conclusion

A series of experiments were conducted to study the effect of octagon-shaped CNF assembly on SMP nanocomposites, of which the actuation was triggered by means of electrically resistive Joule heating. The octagon-shaped CNF assembly improves the electrical property and dynamic mechanical properties, and further effectively optimises heat transfer from CNF assembly to the SMP matrix and temperature distribution in the process of electrical actuation. And the effect of the octagon-shaped CNF assembly on the instinctive structure and dynamic thermomechanical properties of SMP has also been investigated, to characterise their interactions in the SMP nanocomposites. As demonstrated, the electrically driven shape recovery was achieved by means of applying an electric voltage of 3 V, 6 V, 9 V and 10 V, respectively. A simple way has been demonstrated to produce electro-activated SMP nanocomposites by application of deposition of CNF assembly at a porosity of 80%, which enables Joule heating at a low electrical voltage of 10 V.

Acknowledgments

The research reported in this paper was supported by the National Natural Science Foundation of China (NSFC) (Grant No. 51103032) and Fundamental Research Funds for the Central Universities (Grant No. HIT.BRETIV.201304).

Conflict of Interest

The authors declare no conflict of interest.

References

- Bellin, I., Kelch, S., Langer, R. and Lendlein, A. (2006), "Polymeric triple-shape materials", *Proceedings of the National Academy of Science of the United States of America*, Vol. 103 No. 48, pp. 18043-7.
- Behl, M. and Lendlein, A. (2007), "Actively Moving Polymers", *Soft Matter*, Vol. 3, pp. 58-67.
- Choi, M.C., Jung, J.Y. and Chang, Y.W. (2014), "Shape memory thermoplastic elastomer from maleated polyolefin elastomer and nylon 12 blends", *Polymer Bulletin*, Vol. 71 No. 3, pp. 625-35.
- Choi, J.T., Dao, T.D., Oh, K.M., Lee, H.L., Jeong, H.M. and Kim, B.K. (2012), "Shape memory polyurethane nanocomposites with functionalized graphene", *Smart Materials and Structures*, Vol. 21 No. 7, pp. 075017-26.
- Cho, J.W., Kim, J.W., Jung, Y.C. and Goo, N.S. (2005), "Electroactive shape-memory polyurethane composites incorporating carbon nanotubes", *Macromolecular Rapid Communications*, Vol. 26 No. 5, pp. 412-6.
- Dietsch, B. and Tong, T. (2007), "A review-features and benefits of shape memory polymers (SMPs)", *Journal of Advanced Materials*, Vol. 39 No. 2, pp. 3-12.
- Dong, J., Ding, J.B., Weng, J. and Dai, L.Z. (2013a), "Graphene enhances the shape memory of poly (acrylamide-co-acrylic acid) grafted on graphene", *Macromolecular Rapid Communications*, Vol. 34 No. 8, pp. 659-64.
- Dong, Y.B., Ding, J., Wang, J., Fu, X., Hu, H.M., Li, S., Yang, H.B., Xu, C.S., Du, M.L. and Fu, Y.Q. (2013b), "Synthesis and properties of the vapour-grown carbon nanofibre/epoxy shape memory and conductive foams prepared via latex technology", *Composites Science and Technology*, Vol. 76 No. 20, pp. 8-13.
- Fejos, M., Romhány, G. and Karger-Kocsis, J. (2012), "Shape memory characteristics of woven glass fibre fabric reinforced epoxy composite in flexure", *Journal of Reinforced Plastics and Composites*, Vol. 31 No. 22, pp. 1532-7.

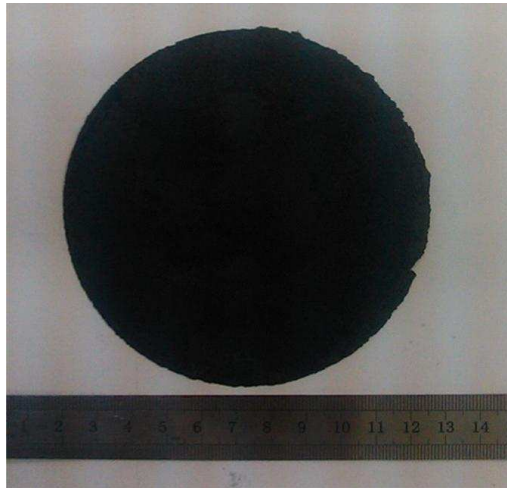
- Gall, K., Kreiner, P., Turner, D. and Hulse, M. (2004), "Shape-memory polymers for microelectromechanical systems", *Journal of Microelectromechanical Systems*, Vol. 13 No. 3, pp. 472-83.
- Hollaway, L.C. (2011), "Thermoplastic-carbon fibre composites could aid solar-based power generation: possible support system for solar power satellites", *Journal of Composites for Construction*, Vol. 15 No. 2, pp. 239-47.
- Huang, W.M., Ding, Z., Wang, C.C., Wei, J., Zhao, Y. and Purnawli, H. (2010), "Shape memory materials", *Materials Today*, Vol. 13 No. 7-8, pp. 54-61.
- Huang, W.M., Yang, B. and Fu, Y.Q. (2011), *Polyurethane Shape Memory Polymers*, CRC Press.
- Hu, J.L. and Chen, S. (2010), "A review of actively moving polymers in textile applications", *Journal of Materials Chemistry*, Vol. 20 No. 17, pp. 3346-55.
- Hu, J.L., Meng, H., Li, G.Q. and Ibekwe, S.I. (2012), "A review of stimuli-responsive polymers for smart textile applications", *Smart Materials and Structures*, Vol. 21 No. 5, p. 053001.
- Kim, B.K., Lee, S.Y., Lee, J.S., Baek, S.H., Choi, Y.J., Lee, J.O. and Xu, M. (1998), "Polyurethane ionomers having shape memory effects", *Polymer*, Vol. 39 No 13, pp. 2803-8.
- Lan, X., Liu, Y.J., Lv, H.B., Wang, X.H., Leng, J.S. and Du, S.Y. (2009), "Fibre reinforced shape-memory polymer composite and its application in a deployable hinge", *Smart Materials and Structures*, Vol. 18 No. 2, pp. 24002-7.
- Lantada, A.D., Morgado, P.L., Sanz, J.L.M., García, J.M., Muñoz-Guijosa, J.M. and Otero, J.E. (2010), "Intelligent structures based on the improved activation of shape memory polymers using Peltier cells," *Smart Materials and Structures*, Vol. 19 No. 5, p. 055022.
- Lee, H.F. and Yu, H.H. (2011), "Study of electroactive shape memory polyurethane-carbon nanotube hybrids", *Soft Matter*, Vol. 7 No. 8, pp. 3801-7.
- Lendlein, A. and Biodegradable, R.L. (2002), "Elastic shape-memory polymers for potential biomedical applications", *Science*, Vol. 296 No. 5573, pp. 1673-6.
- Lendlein, A. (2010), "Progress in actively moving polymers", *Journal of Materials Chemistry*, Vol. 20 No. 17, pp. 3332-4.
- Leng, J.S., Lu, H.B., Liu, Y.J., Huang, W.M. and Du, S.Y. (2009a), "Shape-memory polymers-a class of novel smart materials", *MRS Bulletin*, Vol. 34 No. 11, pp. 848-55.
- Leng, J.S., Lv, H.B., Liu, Y.J. and Du, S.Y. (2007), "Electroactivate shape-memory polymer filled with nanocarbon particles and short carbon fibers", *Applied Physics Letters*, Vol. 91 No. 14, pp. 144105-7.

- Leng, J.S., Wu, X.L. and Liu, Y.J. (2009b), "Infrared light-active shape memory polymer filled with nanocarbon particles", *Journal of Applied Polymer Science*, Vol. 114 No. 4, pp. 2455-60.
- Li, F.K., Qi, L.Y., Yang, J.P., Xu, M., Luo, X.L. and Ma, D.Z. (2000), "Polyurethane/conducting carbon black composites: Structure, electric conductivity, strain recovery behaviour, and their relationships", *Journal of Applied Polymer Science*, Vol. 75 No. 1, pp.68-77.
- Li, S.C., Lu, L.N. and Zeng, W. (2009), "Thermostimulative shape-memory effect of reactive compatibilized high-density polyethylene/poly(ethylene terephthalate) blends by an ethylene-butyl acrylate-glycidyl methacrylate terpolymer", *Journal of Applied Polymer Science*, Vol. 112 No. 6, pp. 3341-6.
- Liu, Y.J., Lv, H.B., Lan, X., Leng, J.S. and Du, S.Y. (2009), "Review of electro-active shape-memory polymer composite", *Composites Sciences Technology*, Vol. 69 No. 13, pp. 2064-8.
- Lu, H.B. (2013), "Comment on Mechanisms of the multi-shape memory effect and temperature memory effect in shape memory polymers by L. Sun and W. M. Huang", *Soft Matter*, 2010, 6, 4403. *Soft Matter*, Vol. 9 No. 47, pp. 11157-8.
- Lu, H.B. and Du, S.Y. (2014), "A phenomenological thermodynamic model for the chemo-responsive shape memory effect in polymers based on Flory-Huggins solution theory", *Polymer Chemistry*, Vol. 5 No. 4, pp. 1155-62.
- Lu, H.B. and Gou, J.H. (2012), "Study on 3-D High Conductive Graphene Buckypaper for Electrical Actuation of Shape Memory Polymer", *Nanoscience and Nanotechnology Letters*, Vol. 4 No. 12, pp. 1155-9.
- Lu, H.B., Gou, J.H., Leng, J.S. and Du, S.Y. (2011a), "Magnetically aligned carbon nanotube in nanopaper enabled shape-memory nanocomposite for high speed electrical actuation", *Applied Physics Letters*, Vol. 98 No. 17, pp. 174105-7.
- Lu, H.B., Gou, J.H., Leng, J.S. and Du, S.Y. (2011b), "Synergistic effect of carbon nanofibre and sub-micro filamentary nickel nanostrand on the shape memory polymer nanocomposite", *Smart Materials and Structures*, Vol. 20 No. 3, pp. 035017-7.
- Lu, H.B. and Huang, W.M. (2013), "Synergistic effect of self-assembled carboxylic acid-functionalized carbon nanotubes and carbon fibre for improved electro-activated polymeric shape-memory nanocomposite", *Applied Physics Letters*, Vol. 102 No. 23, pp. 231910-4.
- Lu, H.B., Huang, W.M. and Yao, Y.T. (2013a), "Review of chemo-responsive shape change/memory polymers", *Pigment & Resin Technology*, Vol. 42 No. 4, pp. 237-46.

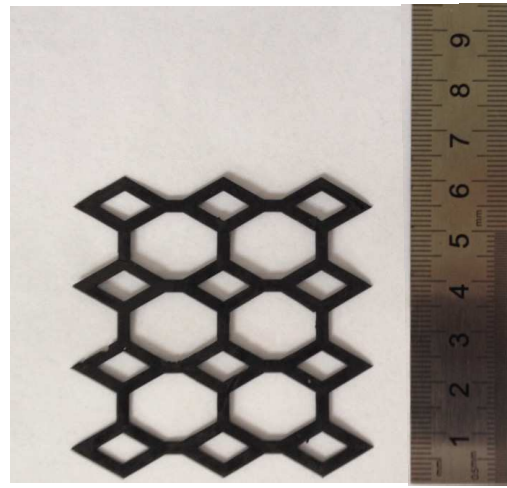
- Lu, H.B., Liang, F. and Gou, J.H. (2011c), "Nanopaper enabled shape-memory nanocomposite with vertically aligned nickel nanostrand: controlled synthesis and electrical actuation", *Soft Matter*, Vol. 7 No. 16, pp. 7416-23.
- Lu, H.B., Liang, F., Yao, Y.T., Gou, J.H. and Hui, D. (2014a), "Self-assembled multi-layered carbon nanofibre nanopaper for significantly improving electrical actuation of shape memory polymer nanocomposite", *Composites Part B: Engineering*, Vol. 59 No. 6, pp. 191-5.
- Lu, H.B., Liu, Y.J., Gou, J.H., Leng, J.S. and Du, S.Y. (2010a), "Synergistic effect of carbon nanofiber and carbon nanopaper on shape memory polymer composite", *Applied Physics Letters*, Vol. 96 No. 8, pp. 084102-4.
- Lu, H.B., Yao, Y.T. and Lin, L. (2013b), "Carbon-based reinforcement in shape-memory polymer composite for electrical actuation", *Pigment & Resin Technology*, Vol. 43 No. 1, pp. 26-34.
- Lu, H.B., Yu, K., Liu, Y.J. and Leng, J.S. (2010b), "Sensing and actuating capabilities of shape memory polymer composite integrated with hybrid filler", *Smart Materials and Structures*, Vol. 19 No. 6, pp. 065014-9.
- Luo, X.F. and Mather, P.T. (2010), "Conductive shape memory nanocomposites for high speed electrical actuation", *Soft Matter*, Vol. 6 No. 10, pp. 2146-9.
- Maitland, D.J., Metzger, M.F., Schumann, D., Lee, A. and Wilson, T.S. (2002), "Photothermal properties of shape memory polymer micro-actuators for treating stroke", *Lasers in Surgery and Medicine*, Vol. 30 No. 1, pp. 1-11.
- Mather, P.T., Luo, X.F. and Rousseau, I. A. (2009), "Shape memory polymer research", *Annual Review of Materials Research*, Vol. 39 No. 1, pp. 445-71.
- Miaudet, P., Derré, A., Maugey, M., Zakri, C., Piccione, P.M., Inoubli, R. and Poulin, P. (2007), "Shape and temperature memory of nanocomposites with broadened glass transition", *Science*, Vol. 318 No. 5854, pp. 1294-6.
- Mohr, R., Kratz, K., Weigel, T., Lucka-Gabor, M., Moneke, M., Lendlein, A. (2006), "Initiation of shape-memory effect by inductive heating of magnetic nanoparticles in thermoplastic polymers", *Proceedings of the National Academy of Sciences*, Vol. 103 No. 10, pp. 3540-6.
- Nguyen, T.D., Qi, J.H., Francisco, C. and Long, K.N. (2008), "A thermoviscoelastic model for amorphous shape memory polymers: Incorporating structural and stress relaxation", *Journal of the Mechanics and Physics of Solids*, Vol. 56 No. 9, pp. 2792-814.

- Paik, I.H., Goo, N.S., Jung, Y.C. and Cho, J.W. (2006), "Development and application of conducting shape memory polyurethane actuators", *Smart Materials and Structures*, Vol. 15 No. 5, pp. 1476-82.
- Razzaq, M.Y., Anhalt, M., Frommann, L. and Weidenfeller, B. (2007), "Mechanical spectroscopy of magnetite filled polyurethane shape memory polymers", *Materials Science and Engineering a-Structural Materials Properties Microstructure and Processing*, Vol. 471 No. 1-2, pp. 57.
- Rousseau, I.A. (2008), "Challenges of shape memory polymers: a review of the overcoming SMP's limitations", *Polymer Engineering Science*, Vol. 48 No. 11, pp. 2075-89.
- Sun, L. and Huang, W.M. (2010), "Mechanisms of the multi-shape memory effect and temperature memory effect in shape memory polymers", *Soft Matter*, Vol. 6 No. 18, pp. 4403-6.
- Sun, L., Huang, W.M., Ding, Z., Zhao, Y., Wang, C.C., Purnawali, H. and Tang, C. (2012), "Stimulus-responsive shape memory materials: a review", *Materials and Design*, Vol. 33, pp. 577-640.
- Tang, Z.H., Sun, D.Q., Yang, D., Guo, B.C., Zhang, L.Q. and Jia, D.M. (2013), "Vapor grown carbon nanofibre reinforced bio-based polyester for electroactive shape memory performance", *Composites Science and Technology*, Vol. 75 No. 19, pp. 15-21.
- Tobushi, H., Hayashi, S., Hoshio, K. and Ejiri, Y. (2008), "Shape recovery and irrecoverable strain control in polyurethane shape-memory polymer", *Science and Technology of Advanced Materials*, Vol. 9 No. 015009, pp. 1-7.
- Tobushi, H., Okumura, K. and Hayashi, S. (2001), "Thermomechanical constitutive model of shape memory polymer", *Mechanics of Materials*, Vol. 33 No. 10, pp. 545-54.
- Xie, T. (2010), "Tunable polymer multi-shape memory effect", *Nature*, Vol. 464 No. 7286, pp. 267-70.
- Yakacki, C.M. and Shandas, R. (2007), "Unconstrained recovery characterization of shape-memory polymer networks for cardiovascular applications", *Biomaterials*, Vol. 28 No. 14, pp. 2255-63.
- Yoonessi, M., Shi, Y., Scheiman, D.A., Lebron-Colon, M., Tigelaar, D.M., Weiss, R.A. and Meador, M.A. (2012), "Graphene polyimide nanocomposites; thermal, mechanical, and high-temperature shape memory effects", *ACS Nano*, Vol. 6 No. 9, pp. 7644-55.

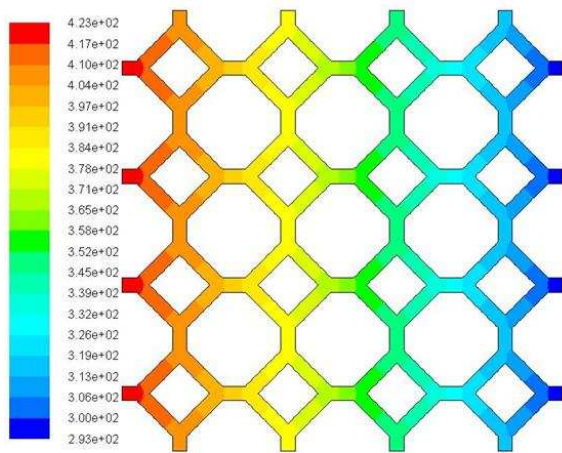
Figure 1 (a) Carbon nanofibre nanopaper, (b) the octagon-shaped CNF specimen, (c) simulation results of heat transfer process, and (d) simulation results of the colour distribution of relative thermal conductivity on the tested specimen by ANSYS FLUENT



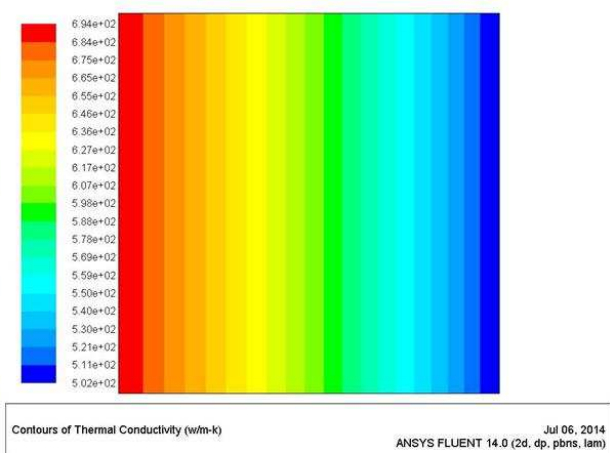
(a)



(b)



(c)



(d)

Figure 2 Relative thermal conductivity of the octagon-shaped CNF assembly with 1 mm, 2 mm and 3 mm width of the skeleton

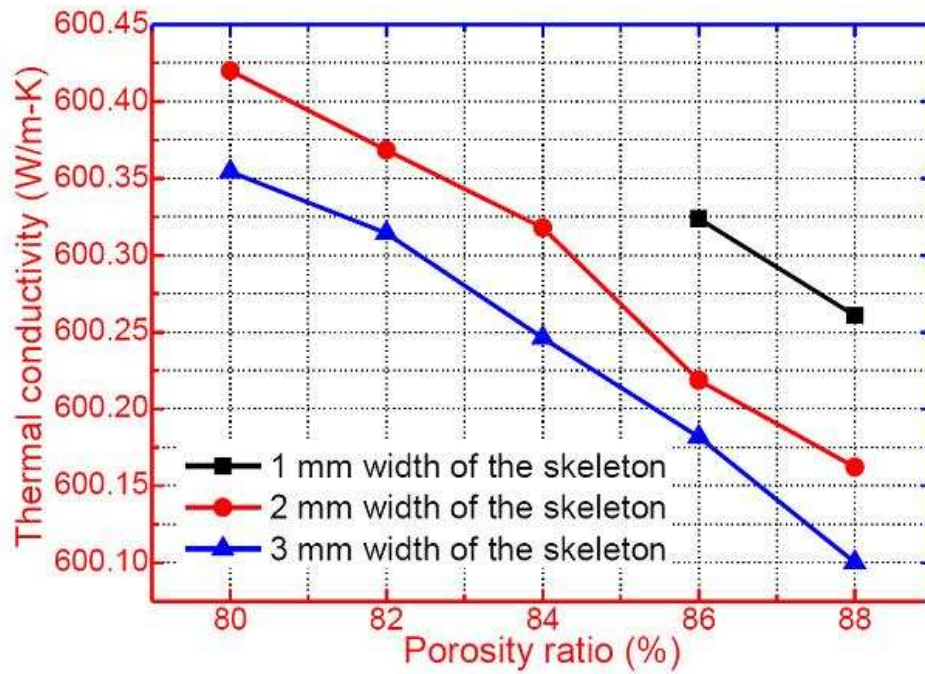


Figure 3 XRD pattern pristine epoxy-based SMP and CNF template enabled SMP nanocomposite in the range of 5-75°

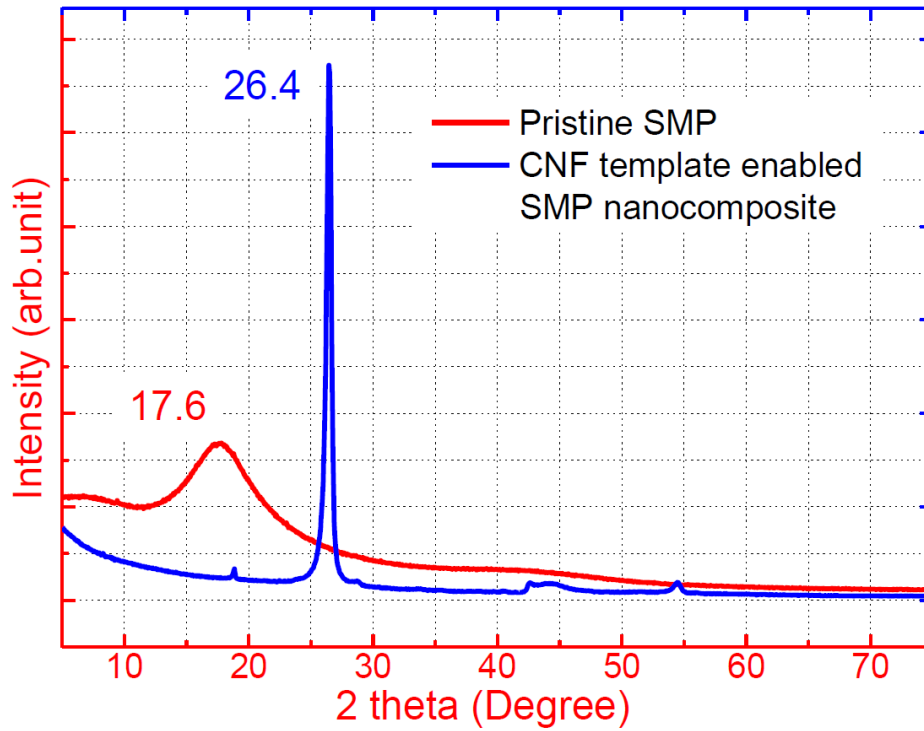


Figure 4 Raman spectra of CNF recorded with 638 nm laser and at a laser power of 1 mW

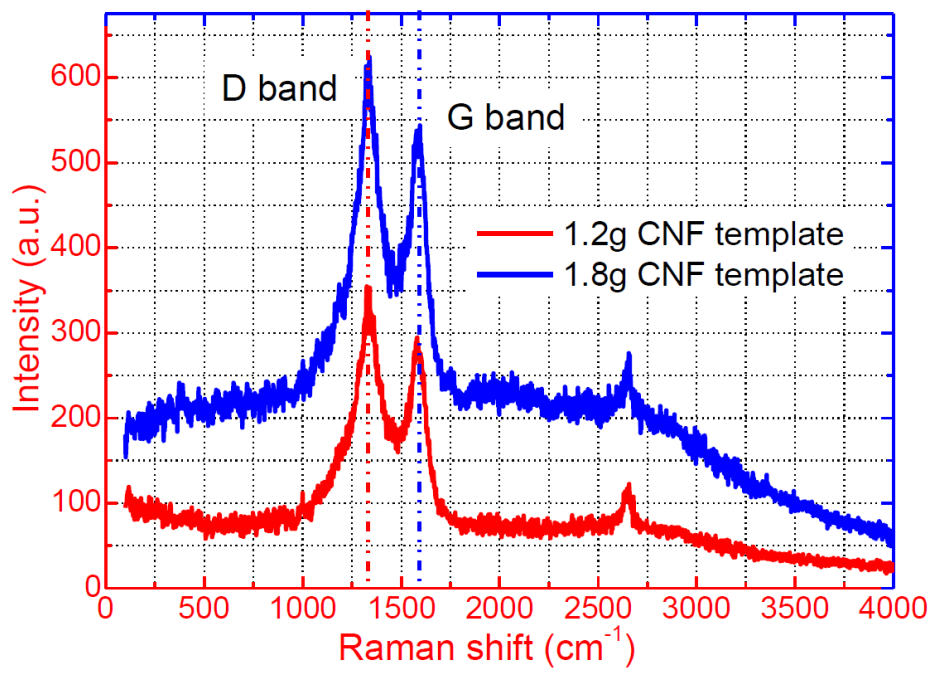


Figure 5 T_g of SMP matrix and SMP nanocomposites incorporated with octagon-shaped CNF assembly with thickness of 0.8 mm and 1.2 mm, respectively

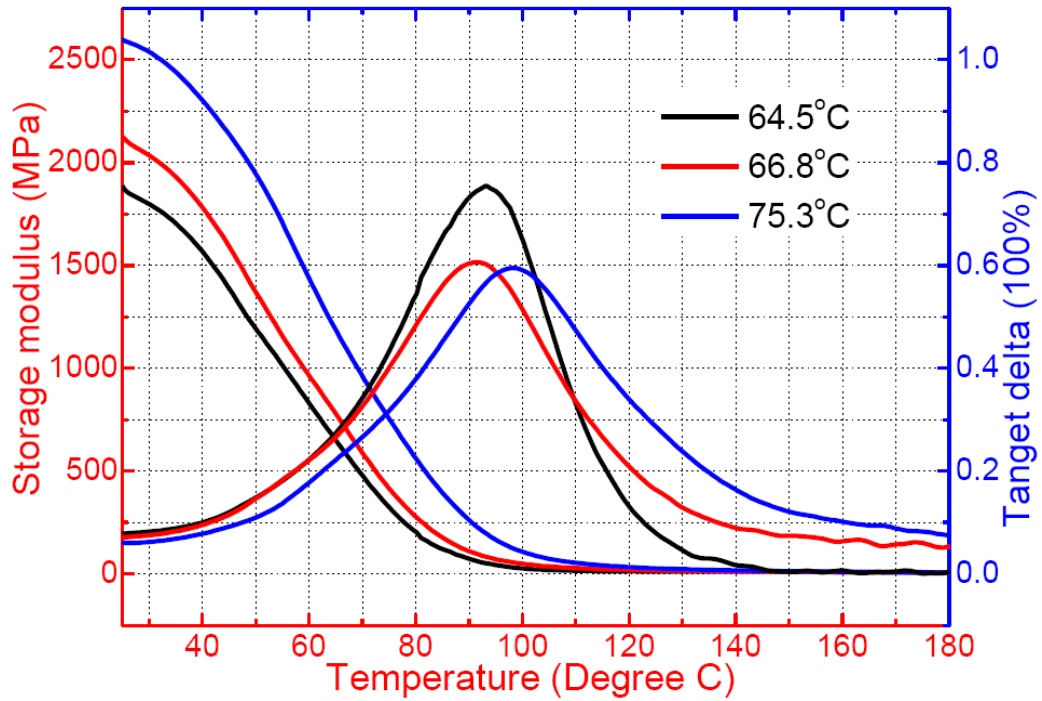


Figure 6 Snapshot of Joule heating and temperature distribution within SMP nanocomposite incorporated with octagon-shaped CNF assembly with skeleton of 2 mm at an applied DC electric voltage of (a) 3 V, (b) 6 V, (c) 9 V and (d) 10 V for 118 s

